Original Article

Institution of MECHANICAL ENGINEERS
Journal of AEROSPACE ENGINEERING

Proc IMechE Part G:
J Aerospace Engineering
2021, Vol. 0(0) 1–12

DOI: 10.1177/09544100211022244
journals.sagepub.com/home/pig
SAGE

Development of a method for maximum structural response prediction of a store externally carried by a jet fighter

Engin Metin Kaplan[1], Erdem Acar[1] and Mehmet Bülent Özer[2]

Abstract

Experimental structural response of equipment mounted in store carried externally by jet type aircraft is investigated, predicted and compared with responses suggested by military standards in this study. A representative store which is similar to Mark-83 warhead with guidance units in terms of mass and geometry is used in this study. The main scope of this study is to evaluate the structural response proposed by military standards with real test conditions and also suggest a new method with an artificial neural network to predict the maximum response. Seventy-five different flight conditions are used to train the network for low and high frequency components. Also, eight flight conditions apart from the training set of flight conditions are used to test the approach. Acceleration levels are collected in real flight conditions by the data storage system. In signal processing, vibration response is expressed as power spectral density functions in the frequency domain. Procedures to predict the maximum response from measurements are determined with statistical limits in the literature. Besides the well-known limits in literature, third-order polynomial normal and logarithmic transform is used, and the performance of the different limits is compared. It is found that the military standard vibration spectrum is conservative. Distribution-free and normal tolerance limits predicted low frequency acceleration spectral density magnitudes more accurately. Their prediction performances were better than those of the other tolerance limits and that of the military standard. Third-order polynomial transform predictions are found to be reasonable with respect to normal prediction limit and envelope approach. Finally, it can be concluded that the response prediction method proposed in this article works well for Mark-83 warheads with guidance unit carried externally by jet fighter.

Keywords

MIL-STD-810, structural response, test spectrum

Date received: 16 April 2021; accepted: 6 May 2021

Introduction

Jet-type aircraft carry electronic warfare pods, missiles, bombs and external fuel tanks. These payloads are exposed to high vibration environment under captive carriage flight conditions.[1] As a result of high vibration conditions, mechanical parts in the object can lose their structural integrity; additionally, electronic cards and circuits can fail. Circuits or components used in aeronautical and space applications also have intermittent defects under severe vibration environments.[2] Vibration tests are performed to verify that the mounted stores can withstand the dynamic loading and continue to function under the expected dynamic conditions.[3] For the selection of subsystems and equipment of the store, such as guidance unit, measurement units, pumps and electronic control units, it is crucial to know the expected vibration levels during the flight in the preliminary design phase of military projects. In some military standards,[4] vibration levels for subsystems are generally estimated on the high side. In these standards,[5] it is advised to avoid using these levels if there is any measurement data. Kin et al[6] examined the military standard levels, compared the vibration levels with the performed measurements and showed that levels given by the military standard were exaggerated. Following these standards may lead to overdesigning of the parts due to their large conservatism of the actual response levels.[7] The disadvantages of using MIL-STD-810 vibration levels are listed below.[8]

[1] Department of Mechanical Engineering, TOBB University of Economics and Technology, Turkey
[2] Department of Mechanical Engineering, Middle East Technical University, Turkey

Corresponding author:
Engin Metin Kaplan, Department of Mechanical Engineering, TOBB University of Economics and Technology, Söğütözü Caddesi No: 43, Çankaya, Ankara 06560, Türkiye.
Email: engin.metin.kaplan@gmail.com

1. Harsh vibration conditions may cause overdesigning of the payloads and its subsystems.
2. Unrealistic failure can occur during tests.
3. It can be difficult to find a test facility that satisfies high vibration exposure.
4. The design period of store can be extended due to unrealistic failure during the tests.
5. Evaluations of aerodynamic dirty (AD) and aerodynamic clean (AC) situations in MIL-STD-810 are difficult to separate.
6. Some explanations of constants in MIL-STD-810 do not cover all store types.

Runyan[9] studied the main vibratory loading sources of a subsystem carried by a jet-type aircraft. Flutter occurs at low frequency regime between 2 and 30 Hz. The frequency bandwidth of the buffet phenomena is higher than flutter. The fluid flow effects can be significant between 100 and 2000 Hz.

Store aircraft interface used in this study is Mau-12 bomb ejector rack. This rack has been designed to provide structural support for external carriage of payloads on aircraft. Two hooks of the store are fixed to two lugs of the aircraft. In addition, sway braces of the aircraft have positive contact with the store in the roll direction.[10] General purpose bombs (Mark-81, Mark-82, Mark-83 and Mark-84) are used against a wide array of threats. A guidance unit with mass representative Mark-83 warhead is used in this study.

Steininger et al[11] found that the most severe vibration occurs about 0.9–0.95 Mach number. The curve of total root mean square 'g' (g-RMS) vs Mach number seems to resemble exponential relation when the flight Mach number is between 0.6–0.9 and 1–1.9. The shape does not change but increases generally when the flight altitude decreases. Corda[12] investigated instrumented pod on F-15 to study vibration levels of both low and high frequency bands. It is seen that vibration levels of the high frequency terms are lower than the low frequency ones in level flight. Sevy et al[13] studied on prediction of vibration spectrums on F-4, F-15 and F-16 parts. When predictions in this reference are investigated, it can be seen that F-16 vibration levels are greater than F-15 in the high frequency range for cockpit electronics. In-flight responses of aerospace equipment are predicted by using flight parameters in the literature. Yildiz[14] predicted flutter behaviour by means of flight parameters. Kutluay et al[15] estimated aerodynamic constants of one-shot autonomous vehicle by flight tests using artificial neural networks (ANN). Mallick et al[16] predicted pressure coefficients of the c-shaped buildings using group method of data handling neural network. Comprehensive experimental study in subsonic wind tunnel is carried out to identify input–output relationship. Mazhar et al[17] estimated longitudinal dynamic behaviour of an airship by nonlinear autoregressive neural network. That network is efficient and reliable for limited flight test data. Results are also validated with previous experimental study conducted with same airship. Quaranta et al[18] identified acoustic signatures of the aeroplanes with ANN. In the procedure, ascending and descending noise of five different aircraft are used. Halle et al[19] predicted moments and forces on the vertical tail plane using in-flight data with local networks. The inputs are taken as the angle of attack, load factors, dynamic pressure, aircraft mass, wing sweep angle and the roll rate. Caliskan et al[20] proposed the method of automatic ice detection and protection system for both military and commercial aircraft by Kalman filter innovation sequence. Neural network trained with estimates of the Kalman filter is used to predict bad-influenced flight dynamic parameters due to icing. Crowther et al[21] estimated flight test flutter speed for four-engined transport aircraft using neural network. In the procedure, an aeroelastic model is used and neural network prediction results are compared with statistical method based on extrapolation of a polynomial fitted to damping data.

There are many studies in the literature which investigate store's structural response due to different types of excitation inputs. Predictions of the spectra in terms of acceleration spectral density (ASD) and frequency in terms of Mach number and flight altitude have not been addressed in the academic literature except military standards. Different from the studies listed above, this study proposes a method to estimate the structural response of equipment in the frequency domain as function of four parameters that are used in military standards. Firstly, power spectral density (PSD) of the acceleration data is calculated. Secondly, tolerance limits are used to indicate conservatism on measured values. Finally, ANN is used to train input–output relationship. The proposed method is also experimentally validated. Vibration testing with electrodynamic shaker on ground is an important issue for experimental validation of complex systems. Performing the vibration tests using the method described in this article as the input rather than military standards can result in cost efficient. In addition, this study can lead future studies for prediction of acoustical noise, shock and pyroshock environments in terms of different input parameters.

The article is structured as follows: In *Theoretical fundamentals*, the theoretical background about random theory, tolerance limits and ANN are given. Also, equations used in MIL-STD-810 are discussed. In *Data collection and tolerance limit estimation*, data management in experimental set-up and usage of tolerance limits are provided. Prediction results are given in *Results*. Conclusion remarks and future studies are discussed in *Conclusion*.

Theoretical fundamentals

Random vibrations

Autocorrelation function can be defined as follows[22]

$$R_{xx}(m) = E\left[x(t)x(t+m)\right] \tag{1}$$

where t is the absolute time, m is the time difference, $x(t)$ is the random process and E is the expected value.

The power spectral density can be derived, as shown in the following equation

$$P_{xx}(f) = \frac{1}{f_s} \sum_{m=-\infty}^{\infty} R_{xx}(m)\ e^{(-j2\pi mf/f_s)} \tag{2}$$

where f denotes the frequency and f_s denotes the sampling frequency.

The mean power of a signal over a designated frequency band can be written as

$$P_{[f_1,f_2\ ]} = \int_{f_1}^{f_2} P_{xx}(f)df \tag{3}$$

where f_1 and f_2 are the lower and the upper frequency values.

Tolerance limits

Tolerance limits are generally used to compensate for the variability in the environment and conditions. Upper tolerance limits add an extra margin to measurement data by estimating excessive upper values due to changes in the environment and conditions. Equipment and systems are designed to endure these loads to ensure they do not fail under operational conditions. The level of conservatism in the upper tolerance limits depends on the coverage and confidence in the parameters.[23]

Descriptions and equations used in calculations of different limits are provided below.

Normal tolerance limit (NTL) is a method used to attain a conservative limit for the structural response spectra. Normal tolerance limit performs only to normally distributed random variables. The spatial variation of structural responses x to excitation is mainly not normally distributed.[24] However, logarithm transformation y of the spectral values has an approximately normal distribution.

Sample average and sample standard deviation are given in equations (4) and (5), respectively

$$\overline{y} = \frac{1}{n}\sum_{i=1}^{n} y_i \tag{4}$$

$$s_y = \sqrt{\frac{1}{n-1}\sum_{i=1}^{n}(y_i - \overline{y})^2} \tag{5}$$

In the above equations, n denotes the sample size and y_i denotes the observed values of sampled items.

NTL_y can be expressed as follows

$$\mathrm{NTL}_y(n,\beta,\gamma) = \overline{y} + k_{n,\beta,\gamma} + s_y \tag{6}$$

The parameter $k_{n,\beta,\gamma}$ is called the normal tolerance factor and is a tabulated parameter. It is a function of β, γ and n which can be found in statistical book references.[25] The degree of conservatism in the upper tolerance limits is determined by the coverage, confidence coefficient and the number of samples which are abbreviated with β, γ and n, respectively.

Reverse logarithmic transformation is needed on NTL of y to get NTL of x. It is given by

$$\mathrm{NTL}_x(n,\beta,\gamma) = 10^{\left(\mathrm{NTL}_y(n,\beta,\gamma)\right)} \tag{7}$$

Distribution-free tolerance limit (DFL) is used to avoid the assumption that the distribution is lognormal. This assumption is overcome by stabilizing the tolerance limit to the maximum spectral value. The main benefit of the distribution-free tolerance limit over the normal tolerance limit is that it does not change with the spatial distribution of the spectral values for the responses within the zone.[26] DFL_x can be expressed as follows

$$\mathrm{DFL}_x(n,\beta,\gamma) = \ x_h, \quad \gamma = 1-\beta^n \tag{8}$$

where x_h is the value that will pass at least the β portion of x_i with a confidence of γ. Calculation of distribution-free tolerance limits is the same as normal tolerance limits, but there is an equation of confidence limit integrated with fraction portion beta.

Normal prediction limit (NPL) is used to yield at a conservative limit for the structural response spectra.[27] Normal prediction limit performs only to normally distributed random variables. Hence, the logarithmic transformation is necessary to get a nearly normal distribution for the transformed spectral values. NPL_y can be written as

$$\mathrm{NPL}_y(n,\gamma) = \overline{y} + \sqrt{1+\frac{1}{n}}\, t_{n-1;a} s_y \tag{9}$$

$$a = 1-\gamma \tag{10}$$

where $t_{n-1;a}$ represents percentage point of Student's t variable and is tabulated in any statistics book.

Reverse logarithmic transformation is also needed on NPL of y to get NPL of x. It is given by

$$\mathrm{NPL}_x(n,\gamma) = 10^{\left(\mathrm{NPL}_y(n,\gamma)\right)} \tag{11}$$

The most prevalent method to calculate at a limit for the structural response spectra within a zone is to apply the spectral responses predicted or measured at n points and then to draw the lines at the maximum spectral values. It does not provide any conservatism to the measurement in terms of tolerance limits. It is called envelope approach (ENV).

Third-order polynomial transform (TPNT) is used for estimating the cumulative distribution function (CDF) of samples in a transformed space. Probit function and the logarithm are used on transformation. Third-order polynomial transform works well with the estimation of quantiles with scarce samples[28]

$$(\zeta_i, F(\zeta_i)) = \left(\zeta_i, \frac{i}{n+1}\right) \tag{12}$$

$$\beta_i = \Phi^{-1}(F(\zeta_i)) \tag{13}$$

The value ζ_i is a set of measurements and $F(\zeta_i)$ is the empirical distribution function. Φ^{-1} is the inverse of the

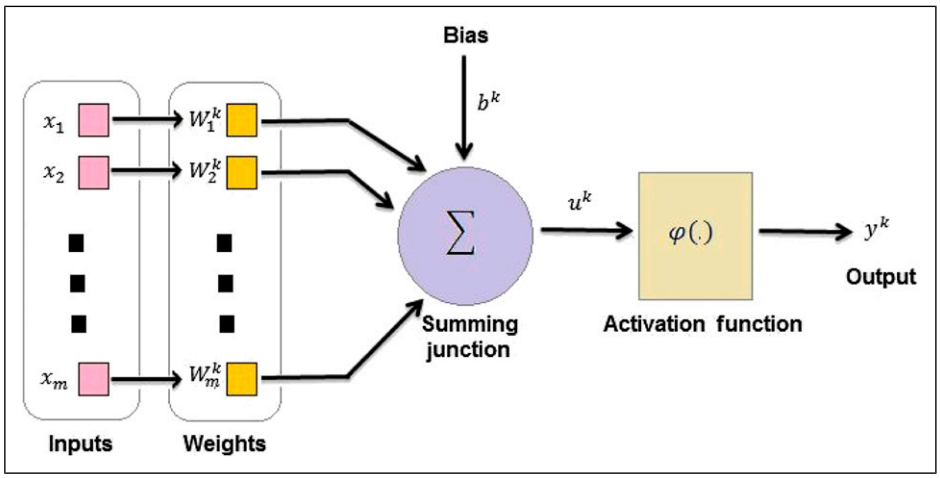

Figure 1. Smoothed envelope options comparison.

standardized distribution function, where β is the reliability index

$$\zeta_i = \sum_{j=0}^{3} \alpha_j \left(\beta_i^j\right) \tag{14}$$

$$\zeta_i = \alpha_0 + \alpha_1 \beta_i + \alpha_2 \beta_i^2 + \alpha_3 \beta_i^3 \tag{15}$$

The monotonicity constraint is achieved as the least square is performed in equation (14). When the cubic polynomial is written as shown in equation (15), monotonicity is achieved by providing the following constraints given

$$\alpha_2^2 + 3\alpha_1\alpha_3 < 0, \quad \alpha_3 > 0 \tag{16}$$

Logarithmic transformation is applied to equation (13) to obtain third-order polynomial logarithmic transform (log-TPNT). $\log \beta_i$ and ζ_i are related as

$$\zeta_i = \sum_{j=0}^{3} \alpha_j \left(\log \beta_i^j\right) \tag{17}$$

The cubic polynomial is written in equation (18), while the monotonicity constraint is provided like TPNT

$$\zeta_i = \alpha_0 + \alpha_1 \log \beta_i + \alpha_2 (\log \beta_i)^2 + \alpha_3 (\log \beta_i)^3 \tag{18}$$

Artificial neural network

Neural networks supply a range of innovative techniques to solve problems in pattern recognition, experimental data analysis and control. They have many significant attributes including high computing speeds and the ability to learn highly nonlinear relationships by its dynamic system response to external inputs.[29] Artificial neural networks come to prominence in tabulated data.[30,31] The ANN in Figure 1 can be expressed by the following equations

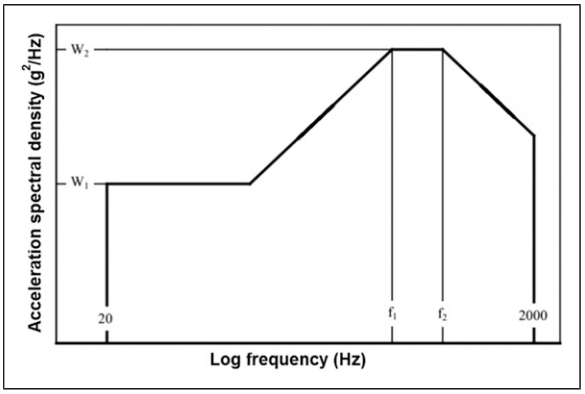

Figure 2. MIL-STD-810 vibration levels for store equipment's.

$$u^k = \sum_{i=1}^{m} w_i^k x_i \tag{19}$$

$$y^k = \varphi\left(u^k + b^k\right) = \varphi\left(\sum_{i=1}^{m} w_i^k x_i + b^k\right) = \varphi\left(\sum_{i=0}^{m} w_i^k x_i\right) \tag{20}$$

Inputs x_i, weights of the inputs w_i^k and summing junctions are three fundamental parts of the neurons in ANN. b^k is called a bias and u^k is a weighted sum of inputs. The output y^k is given by operating on an activation function φ.

Feed forward backprop algorithms are most widely used network with Levenberg–Marquardt implementation in aerospace applications.[32,33] Besides the advantage of its simplicity of training and convergence, it is most prevalent worked network type for prediction of the external loads.[34,35] Hyperbolic tangent sigmoid activation function is used in this study. MATLAB network/data manager tool (nntool) is used for ANN calculations.

MIL-STD-810

MIL-STD-810 is a military specification that indicates vibration levels of the stores which are externally carried by jet-type aircraft under different loading conditions and flight parameters. It is not obvious from the standard that flights were performed with F-16 type aircraft or not. For instance, it is stated that aircraft buffet tests were performed with F-15, but F-16, F-14 and F-18 have the potential to produce buffer vibration.

The suggested vibration level defined in the standard for store equipment carried externally by jet-type aircraft is given in Figure 2. The slope of the curves between W_1-W_2 and W_1-$W_{@2000\ \mathrm{Hz}}$ may be 0 db/octave ±3 db/octave or ±6 db/octave. The vibration levels are described by four parameters: W_1, W_2, f_1 and f_2.[36]

Vibration level parameters W_1, W_2, f_1 and f_2 are calculated as given in equations (21)–(26)

$$W_1 = 0.005 \times K \times A_1 \times B_1 \times C_1 \times D_1 \times E_1 \tag{21}$$

$$W_2 = H \times \left(\frac{q}{\rho}\right)^2 \times K \times A_2 \times B_2 \times C_2 \times D_2 \times E_2 \tag{22}$$

$$\begin{aligned} &M \le 0.90; K = 1, \quad 0.90 \le M \le 1.0; \\ &K = -4.8x \quad M + 5.32, \quad M \ge 1; K = 0.52 \end{aligned} \tag{23}$$

$$q = \left(\frac{1}{2}\right) \times \rho_0 \times \sigma \times V_a^2 \times M^2 \tag{24}$$

$$f_1 = 10^5 \times C \times \left(\frac{t}{R^2}\right) \tag{25}$$

$$f_2 = f_1 + 1000 \tag{26}$$

H in equation (22) and C in (25) are constants and their metric values are 559 and 254, respectively. q is the dynamic pressure at flight conditions given in equation (24). V_a, M, σ and ρ_0 are the local speed of sound (m/s), the Mach number, the ratio of local atmospheric density to sea level atmospheric density and the sea level atmospheric density (kg/m^3), respectively. ρ is the store weight density. The density term ρ is suggested to be kept between 641 and 2403 kg per cubic metre, if it is out of range. t is the load carrying thickness in millimetres and R is the overall store radius in millimetres. Limiting of f_1 values between 100 and 2000 Hz is suggested. Free fall stores f_1 parameter is fixed to 125 Hz in standard. The definitions and values of the parameters A_1, A_2, B_1, B_2, C_1, C_2, D_1, D_2, E_1 and E_2 are given in Table 1. Aerodynamically dirty term indicates the stores that have blunt noses, optical flats, acute corners or deep cavities on its lengths. In this study, A_1, A_2, B_1, B_2, C_1, C_2, E_1 and E_2 are taken as 1. D_1 and D_2 are taken as 8

Table 1. MIL-STD-810[36] parameter definitions and their values.

Parameter definition	Configuration	Parameter 1	Parameter 2
Usage of special adaptor, AC	Single store	A_1: 1	A_2: 1
Usage of special adaptor, AC	Side by side store by adaptor	A_1: 1	A_2: 2
Usage of special adaptor, AC	Behind other store by adaptor	A_1: 2	A_2: 4
Location of the store	Aft half parts of the powered missile	B_1: 1	B_2: 4
Location of the store	Other stores aft half parts	B_1: 1	B_2: 2
Location of the store	Forward parts of the all stores	B_1: 1	B_2: 1
Usage of special adaptor, AD	Single or side by side store by adaptor	C_1: 2	C_2: 4
Usage of special adaptor, AD	Behind other store by adaptor	C_1: 1	C_2: 2
Usage of special adaptor, AD	Other stores	C_1: 1	C_2: 1
Structural mechanics of the store	Production of sheet metal tail cone unit	D_1: 8	D_2: 16
Structural mechanics of the store	Powered missile	D_1: 1	D_2: 1
Structural mechanics of the store	Other stores	D: 4	D_2: 4
Liquid existence in the store	Firebombs including jelly	E_1: 1/2	E_2: 1/4
Liquid existence in the store	Other stores	E_1: 1	E_2: 1

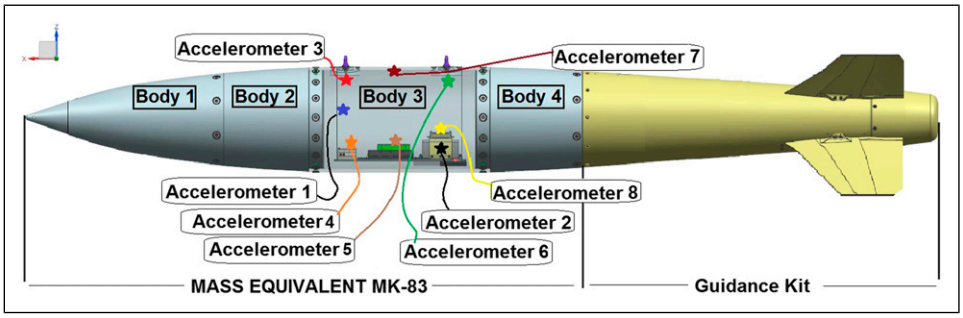

Figure 3. Accelerometer locations on guidance kit.

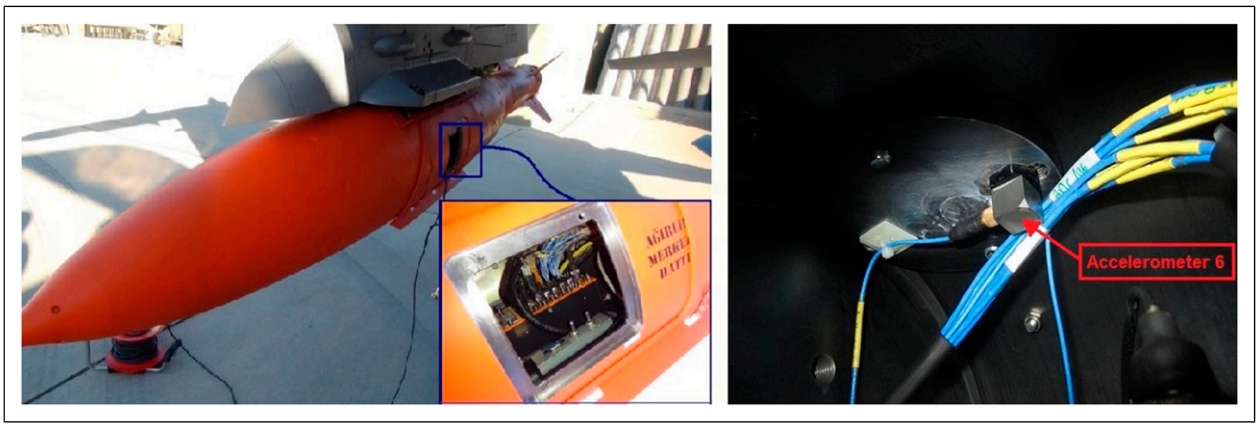

Figure 4. Close view of data storage system and location of accelerometer 6.

Table 2. Accelerometer properties.

Characteristics	Specifications
Full-scale range	±250 g
Sensitivity	20 mV/g
Resolution	0.003 g rms
Natural frequency	38000 Hz

Table 3. Parameter values for tolerance limits.[38]

Method	Parameter	Value
NTL	Beta	0.95
NTL	Gama	0.5
NPL	T Student Gama	0.05
DFL	Beta	0.917
TPNT, Log-TPNT	Beta	0.95

NTL: normal tolerance limit; NPL: normal prediction limit; DFL: distribution-free tolerance limit; TPNT: third-order polynomial transform.

and 16, respectively, since it is a metal fin/tail cone unit. The volume of the store is 0.2 cubic meter.

Data collection and tolerance limit estimation

Instrumentation and data analysis

Considering the cooperation between TÜBİTAK SAGE and Ministry of National Defense, it is possible to work with flight test data of a generic jet fighter aircraft. The data consist of 83 separate aircraft flight conditions. Data contain responses from eight accelerometers on the guidance kit. Eight accelerometers are mounted on equipment of the store by wax. They are positioned between two lugs, as shown with star symbols in Figure 3. All accelerometers are located between suspension lugs in body 3. Accelerometer 1 is placed near the lateral wall of body 3 on the equipment. Accelerometers 2, 4, 5 and 8 are located near the bottom wall on the equipment.

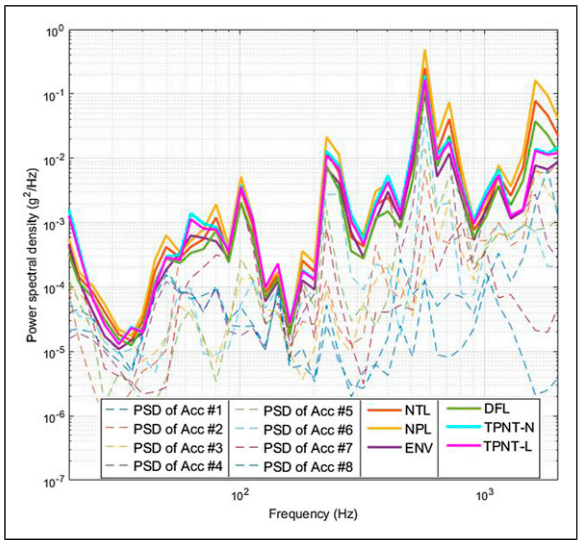

Figure 5. Acceleration spectral density of flight condition 48.

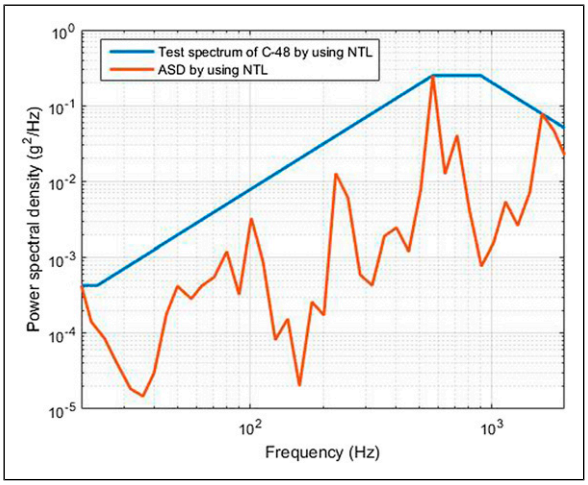

Figure 6. Test spectrum of flight condition 48.

Accelerometers 3 and 6 are located near the suspension lugs on the equipment. Accelerometer 7 is installed on the equipment between suspension lugs. Close view of data storage system and location of accelerometer 6 is given in Figure 4.

The sampling frequency is taken as 10,000 Hz because 20–2000 Hz is considered in aircraft vibration problems. Accelerometer properties are given in Table 2.

Tolerance limit estimation

Constants of tolerance limits used in this study are given Table 3. Accelerations are collected between the altitudes of 12,500 ft and 35,000 ft and between 0.5 and 0.9 Mach numbers. Power spectral density and tolerance limits are calculated using acceleration data. Duration of one second windowed time history data is concerned. 2–1/6 octave band resolution bandwidth is used in spectrums. MATLAB was used to process the collected data.[37] Acceleration spectral density of flight condition 48 in training data and tolerance limits calculated from acceleration data are shown in Figure 5.

W_1 (low frequency amplitude value), W_2 (high frequency amplitude value), f_1 and f_2 are determined for each limit. The shape of the spectra given in Figure 2 is used to

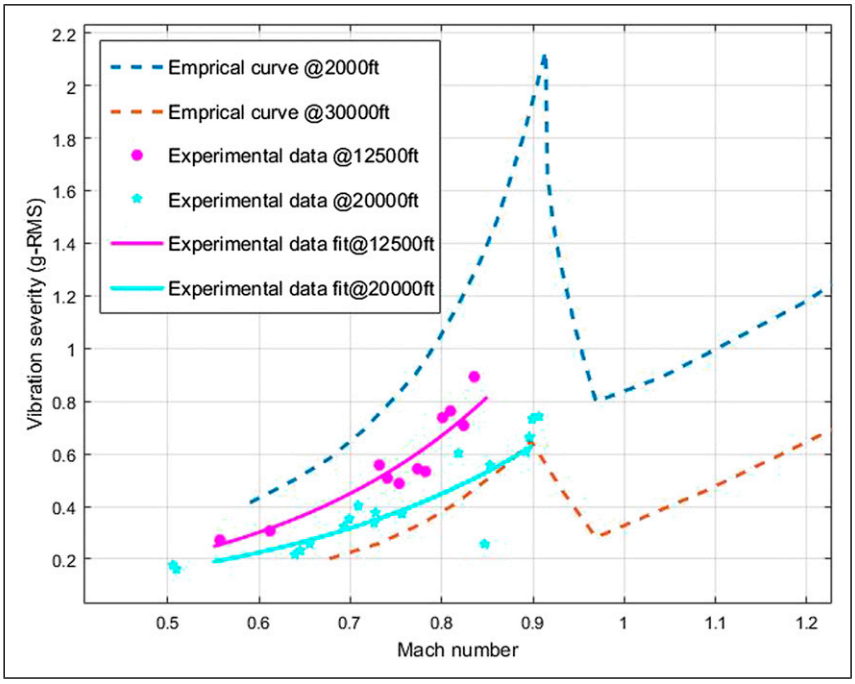

Figure 7. Comparison of experimental and empirical Mach number versus vibration severity at constant attitude.

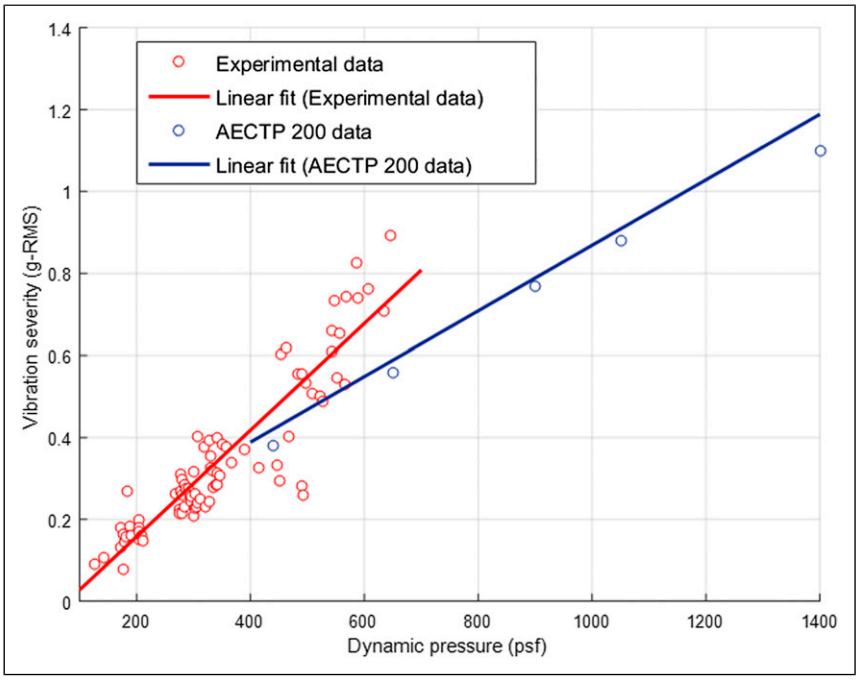

Figure 8. Comparison of experimental and empirical dynamic pressure versus vibration severity.

fit the limits. Vibration spectrum fitted to flight condition 48 with NTL is shown in Figure 6. The envelope is smoothed using a series of straight lines. Usage of maximum seven lines with slopes of 0, ±3 dB/octave and ±6 dB/octave is advised.[39] The smoothed envelope shape is intended to be similar to MIL-STD-810 proposed shape; however, more than one smoothed envelope can be fitted to one specific envelope. In these cases, area under the envelope is minimized since it designates the vibration severity. The approach is given in Supplementary Material.

Table 4. Flight conditions of test cases.

Number	Mach number	Altitude (ft)
1	0.568	13,090
2	0.808	14,513
3	0.699	20,138
4	0.705	31,600
5	0.6	13,573
6	0.783	14,550
7	0.618	24,960
8	0.743	24,960

Results

First, validation of experimental data with literature is demonstrated. Then, data pool in terms of Mach number and flight altitude is mentioned. Finally, tolerance limit comparisons and test case performances are given.

Validation of the data

Vibration severity in terms of g-RMS tends commonly to increase with augmentation of the Mach number.[40] Empirical Mach number versus overall g-RMS relationship[41] is replotted in Figure 7 with experimental data used in this

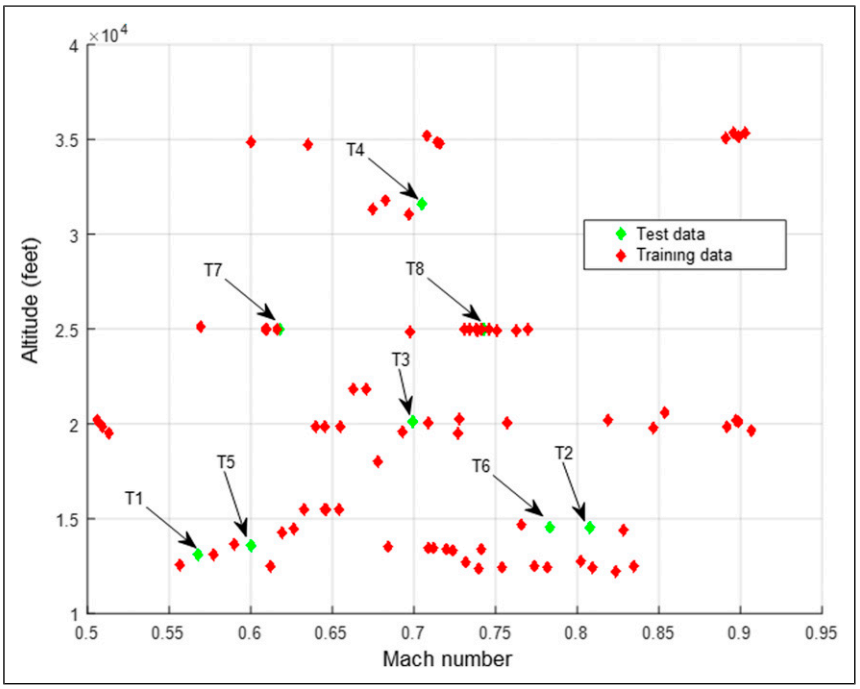

Figure 9. Data pool in Mach number and attitude.

Table 5. Summary of limit performance (mean absolute error).

Tolerance limit	W_1	W_2	f_1	f_2
NTL	17.94	15.04	14.4	25.25
DFL	42.42	23.4	19.45	33.38
NPL	52.98	27.65	25.84	31.47
ENV	42.89	31.36	19.13	32.47
TPNT	46.65	28.45	16.59	28.34
Log-TPNT	34.33	30.86	15.24	30.85

NTL: normal tolerance limit; NPL: normal prediction limit; DFL: distribution-free tolerance limit; ENV: envelope approach; TPNT: third-order polynomial transform.

Table 6. Summary of limit performance (standard deviation of error).

Tolerance limit	W_1	W_2	f_1	f_2
NTL	19.73	12.96	13.65	39.89
DFL	29.04	21.17	20.15	34.67
NPL	80.64	29.27	28.99	49.37
ENV	40.89	28.21	14.03	16.24
TPNT	24.06	24.89	16.55	13.58
Log-TPNT	39.9	28.64	10.63	16.38

NTL: normal tolerance limit; NPL: normal prediction limit; DFL: distribution-free tolerance limit; ENV: envelope approach; TPNT: third-order polynomial transform.

study at 12,500 ft and 20,000 ft. It can be seen that experimental data taken at 12,500 ft and 20,000 ft remain between 2000 ft and 30,000 ft of empirical result curves. Also, increasing trend of vibration severity versus Mach number is similar to empirical data in the literature.

Vibratory loads increase as the dynamic pressure increases.[42] Root mean square vibration is linearly proportional to dynamic pressure.[43] Figure 8 shows that augmentation of dynamic pressure induces more g-RMS level in the store. Graph is replotted with experimental

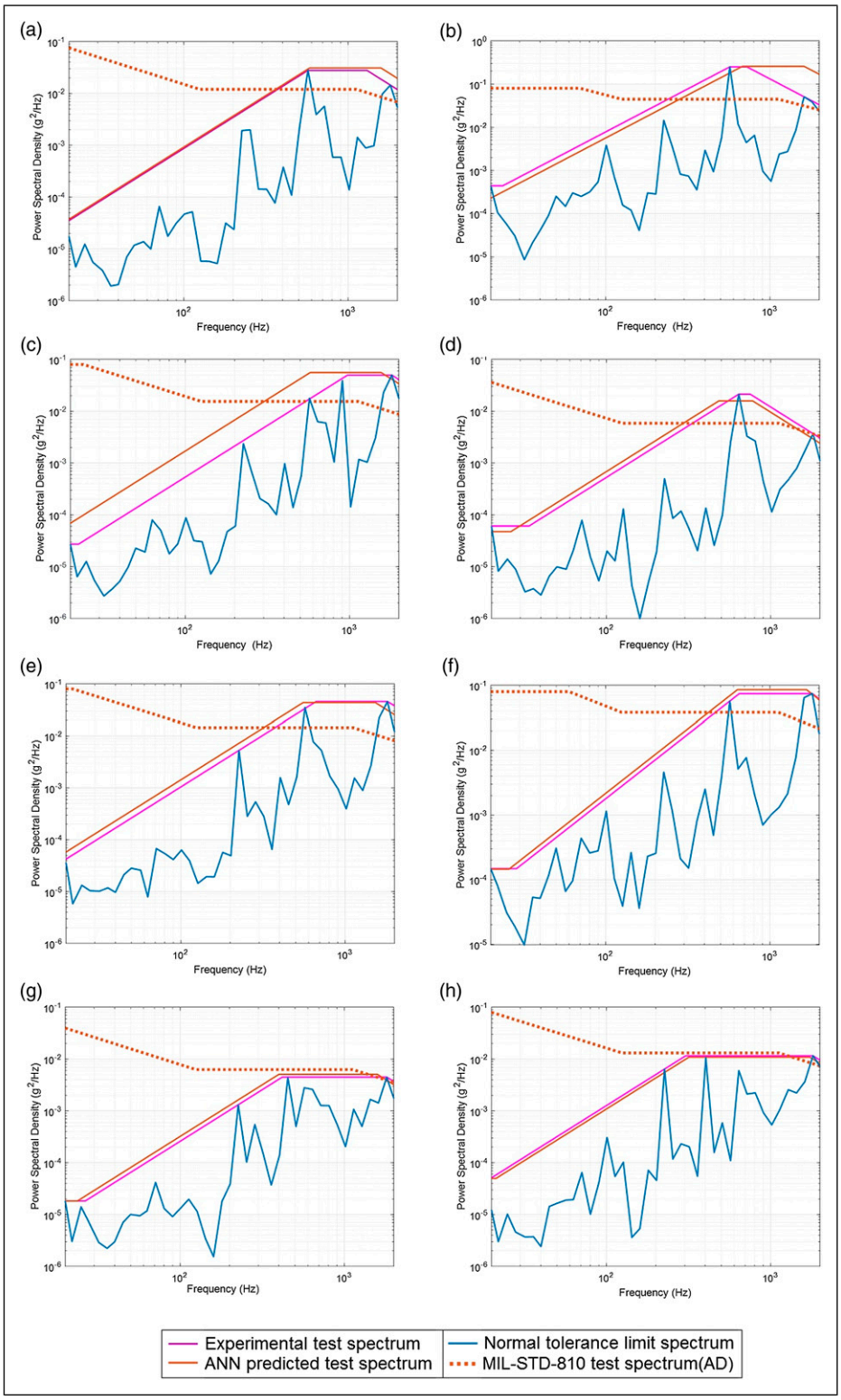

Figure 10. Prediction of normal tolerance limit versus MIL-STD-810: (a) Test case 1; (b) test case 2; (c) test case 3; (d) test case 4; (e) test case 5; (f) test case 6; (g) test case 7; and (h) test case 8.

data.[44] It is seen that there is a good agreement between literature and experimental results.

Training and test sets of flight conditions

Test set of flight condition is given in Table 4. In addition, Figure 9 shows the location of the training and test points in the Mach number–altitude variable space. Green points are indicated as test cases.

Tolerance limit comparison

Summary of the limit performance can be seen in Tables 5 and 6. Generally W_2 predictions are more accurate than W_1 in all limits. Normal tolerance limit results have the lowest error percentage among limits. Distribution-free tolerance limit works well on W_2 prediction after NTL. Predictions of log-TPNT on W_1 and TPNT on W_2 showed that these methods are second or third among other methods according to the arrangement of least mean error.

Mean absolute error of NTL test results are 17.94 for W_1, 15.04 for W_2, 14.48 for f_1 and 25.25 for f_2. Distribution-free tolerance limit, NPL and ENV in literature are tested with ANN. It is seen that DFL is more accurate in W_1 and W_2 prediction rather than NPL and ENV. The limits used in scarce sample TPNT and log-TPNT transform are also tested with ANN training network. It is seen that log-TPNT performance is better than DFL, NPL and ENV on W_1 prediction. Performance of TPNT and log-TPNT is reasonable compared to other limits for the remaining parameters W_2, f_1 and f_2. Results of the individual test cases for the limits are given in Supplementary Material.

ANN performance on test cases

Eight different test points are randomly selected from Mach number–altitude space to validate the performance of the ANN predictions. Artificial neural network–predicted test spectrum is compared to the experimental test spectrum. Moreover, the results of the MIL-STD-810 are compared with experimental results. Military standard levels are given as AD case that uses the parameters C_1 and C_2 as 2 and 4, respectively.

Figure 10 shows that NTL prediction test spectrums are more accurate than MIL-STD-810 AD on all test cases. Also, structural response estimations based on MIL-STD-810 are conservative, especially for low frequency between 20 Hz and 125 Hz range. High frequency amplitude of PSD (W_2) based on MIL-STD-810 is found to be more accurate than W_1, in particular for the test cases 7 (T7) and 8 (T8). MIL-STD-810 AD covers singular accelerometer measurements except test case 2. Some individual accelerometer responses at high frequency band exceed MIL-STD-810-AD prediction. They are local overflows in a narrow band, and the results of MIL-STD-810 AD are generally found to be highly conservative, especially for the low frequency range.

W_1 values are greater than W_2 values in all cases based on MIL-STD-810 calculations. W_2 value is inversely proportional to the square of the density of the store. The density of the instrumented pod is high due to its steel material property, and it may be the reason for the lower value of W_2 according to W_1 at MIL-STD-810 predictions. MIL-STD-810 also fixes the frequency bands for free fall stores to 125 Hz and 1125 Hz, respectively. Frequency values are predicted more accurately than MIL-STD-810 by the proposed method.

Conclusion

The present article introduced a new method for the prediction of the structural response of equipment inside the store in terms of Mach number and flight altitude. It was found that MIL-STD-810 exhibited conservatism on equipment vibration response, especially in the low frequency region.

The proposed prediction strategy also involves safety factor by using tolerance limits. Performances of limits were compared with each other. An artificial neural network was used to train 75 flight conditions. In order to demonstrate its merit, 8 test cases apart from training data were studied to check the ANN prediction performance. Firstly, NTL results showed that structural response could be predicted by the proposed method. It should be noted that, all frequency and ASD predictions in the proposed approach are better than military standard estimates. Moreover, the structural response was predicted in terms of four parameters in the frequency domain, contrary to similar studies which predicts g-RMS value of ASD-frequency curve. Secondly, different limit performances were compared through test cases. Two new limits, third-order polynomial subjected to monotonicity constraint with normal and logarithmic transforms, were tested in structural response prediction. It was seen that new limit results were not as good as NTL, but they provided acceptable results.

The proposed method can be implemented to any store that is suspicious whether the outer geometry is AD or not. AD case depends on separated aerodynamic flow according to MIL-STD-810. The proposed method is sensitive to the aerodynamic characteristics of any store.

As for future work, the concept of application of the method can be implemented on different output predictions as shock and acoustic noise in terms of input parameters.

Acknowledgements

The authors acknowledge the contribution of TÜBİTAK SAGE, Turkey, which provided the raw accelerometer data collected from a jet fighter.

Declaration of Conflicting Interests

The author(s) declared no potential conflicts of interest with respect to the research, authorship and/or publication of this article.

Funding

The author(s) received no financial support for the research, authorship and/or publication of this article.

ORCID iDs

Engin Metin Kaplan https://orcid.org/0000-0002-8576-4071
Erdem Acar https://orcid.org/0000-0002-3661-5563

Supplementary Material

Supplementary material for this article is available online.

References

1. Hall PS. *Vibration test level criteria for aircraft equipment*. OH, USA: Air Force Wright Aeronautical Lab Wright-Patterson AFB, 1980.
2. Guanjun L, Hui Z, Jing Q, et al. Mechanism of intermittent failures in extreme vibration environment and online diagnosis technology. *Proc Inst Mech Eng G: J Aerosp Eng* 2015; 229(13): 2469–2480.
3. Jang J and Park J-W. Simplified vibration PSD synthesis method for MIL-STD-810. *Appl Sci* 2020; 10(2): 458.
4. Nevius H and Brignac W. Dynamic qualification testing of F-16 equipment. *AGARD Dyn Environ Qualification Tech* 1981; 15: 5–9.
5. Das BK and Kumar P. Tailoring of specifications for random vibration testing of military airborne equipments from measurement. *Int J Res Eng Technol* 2015; 4(12): 293–299.
6. Kim J, Park S, Eun W, et al. Vibratory loads and response prediction for a high-speed flight vehicle during launch events. *Int J Aeronaut Space Sci* 2016; 17(4): 551–564.
7. Chung Y, Krebs D and Peebles J. Estimation of payload random vibration loads for proper structure design. In: 19th AIAA Applied Aerodynamics Conference, Anaheim, CA, 11–14 June 2001, p. 1667.
8. Lalanne C. *Mechanical vibration and shock analysis, specification development*. Paris, France: John Wiley & Sons, 2013.
9. Runyan HL. Some recent information on aircraft vibration due to aerodynamic sources. *J Acoust Soc Am* 1968; 44: 364.
10. AGARDograph S and Series-Volume FTT. *Aircraft/stores compatibility, integration and separation testing*. Brussels, Belgium: NATO: S&T Organization, 2014.
11. Steininger M and Haidl G. Vibration qualification of external A/C stores and equipment. *AGARD Dyn Environ Qualification Tech* 1981; 14.
12. Corda S. *In-flight vibration environment of the NASA F-15B flight test fixture*. CA, USA: NASA Dryden Flight Research Center, 2002.
13. Sevy RW and Haller MN. *Computer program for vibration prediction of fighter aircraft equipments*. OH, USA: Air Force Flight Dynamics Lab Wright-Patterson AFB, 1977.
14. Yıldız EN. *Aeroelastic stability prediction using flutter flight test data*. Ankata, Turkey: METU, 2007.
15. Kutluay U, Mahmutyazicioglu G and Platin B. An application of equation error method to aerodynamic model identification and parameter estimation of a gliding flight vehicle. In: AIAA atmospheric flight mechanics conference, Chicago, IL, 10–13 August 2009, p. 5724.
16. Mallick M, Mohanta A, Kumar A, et al. Prediction of wind-induced mean pressure coefficients using GMDH neural network. *J Aerospace Eng* 2020; 33(1): 04019104.
17. Mazhar F, Choudhry MA and Shehryar M. Nonlinear autoregressive neural network for mathematical modelling of an airship using experimental data. *Proc Inst Mech Eng Part G: J Aerosp Eng* 2019; 233(7): 2549–2569.
18. Quaranta V and Dimino I. Experimental training and validation of a system for aircraft acoustic signature identification. *J Aircr* 2007; 44(4): 1196–1204.
19. Halle M and Thielecke F. Flight loads estimation using local model networks. In: 29th congress of the international council of the aeronautical sciences, St. Petersburg, Russia, 7–12 September 2014.
20. Caliskan F, Aykan R and Hajiyev C. Aircraft icing detection, identification, and reconfigurable control based on Kalman filtering and neural networks. *J Aerosp Eng* 2008; 21(2): 51–60.
21. Crowther WJ and Cooper JE. Flight test flutter prediction using neural networks. *Proc Inst Mech Eng Part G: J Aerosp Eng* 2001; 215(1): 37–47.
22. Newland DE. *An introduction to random vibrations, spectral & wavelet analysis*. NY, USA: Courier Corporation, 2012.
23. Edwards TS. Probability of future observations exceeding one-sided, normal, upper tolerance limits. *J Spacecr Rockets* 2015; 52(2): 622–625.
24. Hughes WO and Paez TL. *Application of the bootstrap statistical method in deriving vibroacoustic specifications*. CA, USA: NASA, 2006.
25. Bethea RM and Rhinehart RR. *Applied engineering statistics*. FL, USA: CRC Press, 1991, Vol. 121.
26. Wang C, Bai J, Wan F, et al.. Review of statistical induction analysis methods on aircraft vibration test data. *Proced Environ Sci* 2011; 10: 825–830.
27. Gibbons RD, Bhaumik DK and Aryal S. *Groundwater monitoring, detection, and compliance*. NJ, USA: Wiley StatsRef: Statistics Reference Online, 2014.
28. Ramu P and Arul S. Estimating probabilistic fatigue of Nitinol with scarce samples. *Int J Fatigue* 2016; 85: 31–39.
29. Paksoy A and Aradag S. Artificial neural network based prediction of time-dependent behavior for lid-driven cavity flows. *Isi Bilimi ve Teknigi Dergisi/Journal Therm Sci Technol* 2015; 35(2): 1–18.
30. Zhen Z, Liu J, Zhang Z, et al. Deep learning based surface irradiance mapping model for solar PV power forecasting using sky image. *IEEE Trans Industry Appl* 2020; 56(4): 3385–3396.
31. Yang C, Jiang W and Guo Z. Time series data classification based on dual path CNN-RNN cascade network. *IEEE Access* 2019; 7: 155304–155312.
32. Sharan A, Vijayaraju K and James D. Synthesis of in-flight strains using flight parameters for a fighter aircraft. *J Aircr* 2013; 50(2): 469–477.
33. Winter M and Breitsamter C. Nonlinear identification via connected neural networks for unsteady aerodynamic analysis. *Aerosp Sci Technol* 2018; 77: 802–818.
34. Durodola JF, Li N, Ramachandra S, et al.. A pattern recognition artificial neural network method for random fatigue loading life prediction. *Int J Fatigue* 2017; 99: 55–67.
35. Durodola JF, Ramachandra S, Gerguri S, et al. Artificial neural network for random fatigue loading analysis including the effect of mean stress. *Int J Fatigue* 2018; 111: 321–332.
36. Thompson MK. *MIL-STD-810G environmental engineering considerations and laboratory tests*. Washington, USA: US Department of Defense, 2008.

37. Schmid H. How to use the FFT and Matlab's pwelch function for signal and noise simulations and measurements. *FHNW/IME* 2012: 2–13.
38. Keegan WB. *Dynamic environmental criteria (NASA report# HDBK-7005) NASA technical handbook*. CA, USA: NASA, 2001.
39. Piersol AG. Procedures to compute maximum structural responses from predictions or measurements at selected points. *Shock Vib* 1996; 3(3): 211–221.
40. Dreher JF. *Aircraft equipment random vibration test criteria based on vibrations induced by turbulent airflow across aircraft external surfaces*. OH, USA: Air Force Flight Dynamics Lab Wright-Patterson AFB, 1983.
41. Wafford J, Haidl G, Lodge Cet al. *Dynamic environmental qualification techniques*. Neuilly Sur Seine, France: Advisory Group fir Aerospace Research and Development Neuilly-Sur-Seine (France), 1979.
42. Kartman A. Emprical prediction of missile flight random vibrations. *Shock Vib Bull* 1970; 41: 4.
43. Cap JS, C De Baca MK and Skousen TJ. *The derivation of maximum predicted environments for externally carried stores using a small number of flight tests*. Albuquerque, NM: Sandia National Lab.(SNL-NM), 2014.
44. Maj J. *Allied environmental conditions and test publications, AECTP 200*. Brussels, Belgium: NATO Standardisation Agency (NSA), 2006.